

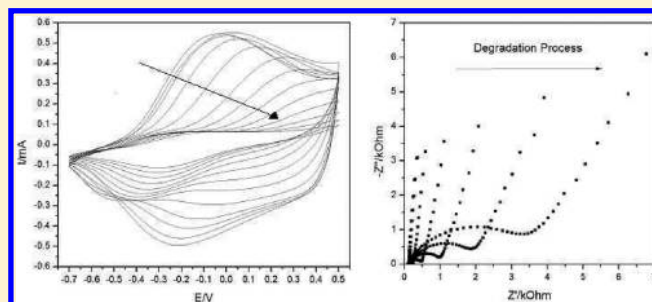
# Investigation of Polypyrrole Degradation Using Electrochemical Impedance Spectroscopy

L. F. Q. P. Marchesi,<sup>†</sup> F. R. Simões,<sup>‡</sup> L. A. Pocrifka,<sup>†</sup> and E. C. Pereira<sup>\*,†</sup>

<sup>†</sup>Laboratório Interdisciplinar de Eletroquímica e Cerâmica, Centro Multidisciplinar para o Departamento de Química, Universidade Federal de São Carlos, Caixa Postal 676, CEP 13565-905 São Carlos, SP, Brazil

<sup>‡</sup>Departamento de Ciências Exatas e da Terra, UNIFESP, CEP 09972-270, Diadema, SP, Brazil

**ABSTRACT:** In this paper, the electrochemical degradation of polypyrrole film was studied by means of overpotential application. The overpotential was 0.58 V versus SCE, and after every 5 min of application of 0.58 V, a cyclic voltammogram was recorded in the range of  $-0.7$  to  $0.5$  V as well as an electrochemical impedance spectroscopy and electrochemical quartz crystal microbalance (EIS and EQCM). The main characteristic is the huge increase in the charge transfer resistance ( $r_{ct}$ ), which indicates that the insertion process of ions in the polymer matrix is hindered by the electrochemical degradation. Once the process of insertion is damaged, the number of intercalated ions in the matrix should decrease, which is expressed by the low-frequency capacitance, which is proportional to the number of intercalated ions in the polymeric matrix. The decrease of intercalated ions has an influence in the mass variation of the polymer film, which is confirmed by EQCM measurements.



## 1. INTRODUCTION

One of the most extensively studied and used polymers has been polypyrrole (Ppy), due to its high electrical conductivity and good environmental stability. It can be polymerized by chemical or electrochemical methods, and, in both cases, the material is obtained in the oxidized (doped) high-conductivity state. However, the main drawback of polypyrrole materials is that they undergo irreversible electrochemical degradation under anodic potentials and become insulator after several redox cycles.<sup>1,2</sup> In this sense, electrochemical degradation represents an irreversible change that occurs upon anodic polarization leading to an irreversible decrease in its redox activity and/or electronic conductivity. Such kind of polarization is also called overoxidation.<sup>3</sup> As early as 1982, Bard et al. found that some irreversible overoxidation of Ppy occurred at potentials higher than 0.6 V versus SCE.<sup>4</sup> Later, Beck et al. studied the effect of nucleophiles ( $\text{OH}^-$  and  $\text{Br}^-$ ) on the overoxidation and found that the presence of a strong nucleophile as  $\text{OH}^-$  leads to the quinone formation that disrupt the conjugated system and, hence, damage the electronic and electrochemical properties of oxidized polypyrrole.<sup>5,6</sup> Schlenoff et al. investigated the overoxidation process by EQCM and proposed that this reaction is accompanied by mass loss in the polymer.<sup>7</sup> Ge et al. measured XPS spectra of Ppy before and after overoxidation and found that the  $\beta$ -C of pyrrole was oxidized to C=O during the overoxidation.<sup>8</sup> Another important characteristic of the overoxidized conducting polymer is that the polymer is in a dedoped state; i.e., the anions are expelled from the polymer.<sup>2</sup> However, the mechanism of overoxidation still remains unclear and the

irreversible structure change after overoxidation needs to be clarified further. For this reason, the degradation process of conducting polymers has been studied extensively using techniques including electrochemical impedance spectroscopy (EIS), chronoamperometry, and spectroscopic methods.

The analysis of impedance data could be subject to different interpretations as a result of the possible selection from different available impedance models. This degree of uncertainty is not only due to the number of electrical effects that take place in any electrochemical system but it can arise also from the different possible approach to describe the mechanism underlying these reactions. Using equivalent circuit to interpret impedance data, there are two basic approaches concerning the electrochemical response of polymeric films. The first one assumes that the electroactive film is a homogeneous structure in which the macroscopic boundary between the film and the electrolyte plays a central role.<sup>9,10</sup> In this view, ionic transport is modeled by means of diffusion along the polymer bulk. The second proposition, called distributed impedance model, highlights the porous nature of these films and, according to this, distributes the polymer/electrolyte interface inside the electrode matrix.<sup>11–13</sup> Charge transport and polarization (both in the polymer chains and in the electrolyte inside the pore) and a highly complex interfacial structure yield, in most cases, complex impedance spectra.

Received: May 4, 2011

Revised: June 27, 2011

Published: July 01, 2011

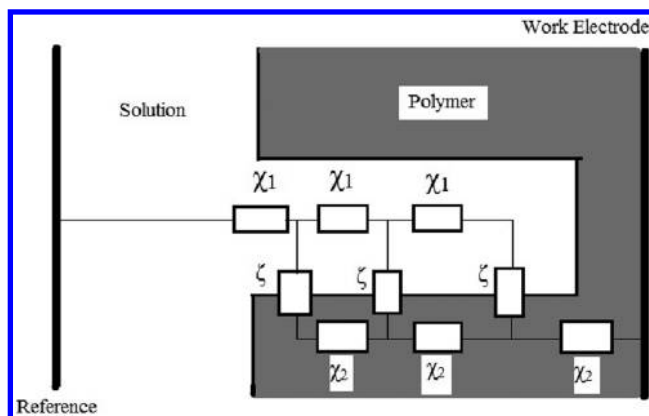


**Figure 1.** Scheme of a generic porous electrode showing the distributed impedances discussed in the text.

In the distributed model, the material operates in contact with an electrolyte by simultaneous transport of electronic and ionic species in the solid and liquid phases, respectively. The solid phase in contact with the conducting substrate provides a continuous path for the transport of electrons (or holes) in a nanometer dimension. The electrolyte penetrates the voids in the solid phase that have a quite small dimension. Therefore, the system is characterized by the existence of two closely mixed phases in the electroactive layer, with narrow channels for transport. Considering these facts, a dual-channel transmission line model has been adopted by different authors to describe the electrochemical behavior of conducting polymers.<sup>14,15</sup> The classical model for a porous or mixed-phase electrode of thickness  $L$  gives rise to the following impedance function

$$Z = \frac{\chi_1 \chi_2}{\chi_1 + \chi_2} \left( L + \frac{2\lambda}{\sinh(L/\lambda)} \right) + \lambda \frac{\chi_1^2 + \chi_2^2}{\chi_1 + \chi_2} \coth(L/\lambda) \quad (1)$$

where

$$\lambda = \left( \frac{\zeta}{\chi_1 + \chi_2} \right)^{1/2} \quad (2)$$

and is schematically represented in Figure 1. Subscripts 1 and 2 denote the liquid and solid phase, respectively. The quantities  $\chi_1$  and  $\chi_2$  represent impedance per unit length ( $\Omega \text{ m}^{-1}$ ) transverse to the macroscopic outer surfaces, corresponding to the whole electrode area. On the other hand,  $\zeta$  represents an impedance length ( $\Omega \text{ m}$ ) parallel to the macroscopic surface, describing both faradaic current and polarization at the distributed interface.<sup>16</sup>

When the polymer is kept in the oxidized conducting state, one can effectively assume that  $\chi_1 \gg \chi_2$ , and thus  $\chi_2 \approx 0$ ; the charge transport is then mainly determined by the ionic species in the pores because the polymeric phase is viewed basically as an equipotential. When transport features in both phases yield comparable behavior, it is often difficult to interpret experimental data unambiguously.<sup>17</sup> In this case the elements  $\chi_1$  and  $\chi_2$  may not correspond to simple resistive responses.<sup>16</sup>

Interpretation of the behavior of the materials as a function of the anodic polarization time in the overoxidation region is more complex to analyze as changes in the oxidation state once this last

ones can cause drastic changes in the electrochemical properties of conducting polymers. Also, the concentration of ions in the polymer causes structural changes that likely affect the porosity of the film and the diffusivity of the ions.<sup>18</sup>

The properties of conducting polymers are directly linked to their oxidation state, which can be controlled by electrochemical oxidation/reduction processes. It has been suggested that, during electrochemical polarization, several processes could occur: electron transfer between the electrode and the film, electron and/or ion transport in the film, ion transfer between the solution and the film, and ion transport and diffusion of ions in the pore solution. The understanding of such effects related to the charge compensation mechanism has not yet been accomplished and it is considered as essential to develop electrochemical devices. In addition, the apparent kinetic is controlled by the slowest process among those mentioned above.<sup>19</sup> In this context, to build electrochemical devices, their behavior upon several electrochemical cycles which, many times, include anodic polarization in the degradation region (overoxidation) must be understood.

Considering the exposed above, the purpose of this paper is to study, through EIS and EQCM (electrochemical quartz crystal microbalance), the degradation process of Ppy films by overoxidation. Transmission line models will be used to better understand processes such as transfer of electrons between the electrode and the conducting polymer, transport of ions in the polymer, and transfer of ions from the solution to or from the film to maintain charge neutrality by compensating the positive charges formed (e.g., polarons) in the film when it is oxidized.

## 2. EXPERIMENTAL SECTION

All chemicals were of analytical grade. Pyrrole (Sigma) was distilled before use. All solutions were prepared in reverse osmosis water. Ppy was electrochemically prepared from aqueous solutions of  $0.1 \text{ mol L}^{-1}$  monomer and  $0.1 \text{ mol L}^{-1}$   $\text{LiClO}_4$  (Alfa Aesar) as supporting electrolyte. Following this, films were removed from the solution and washed in distilled water, dried in air, and transferred to an aqueous solution of  $0.1 \text{ mol L}^{-1}$   $\text{LiClO}_4$  in which electrochemical experiments were performed. All the experiments were performed at  $25^\circ \text{C}$ .

Electropolymerization was performed on a platinum disk electrode ( $A = 0.20 \text{ cm}^2$ ), under potentiostatic conditions ( $0.75 \text{ V}$  versus saturated calomel electrode SCE) until the passed charge reached  $80 \text{ mC cm}^{-2}$ . A platinum electrode was used as auxiliary electrode. At this grown potential, the as-prepared films had undergone overoxidation to some extent, but we consider this negligible when compared to the degradation process conditions used to promote the loss of the electrochemical properties of the polypyrrole film.

Cyclic voltammetry (CV) was carried out at a scan rate of  $50 \text{ mV s}^{-1}$  from  $-0.7$  to  $0.5 \text{ V}$  versus SCE. The measurements of electrochemical impedance spectroscopy (EIS) were carried out at  $0.3 \text{ V}$  at different times of overoxidation, and the frequency range was from  $10 \text{ kHz}$  to  $10 \text{ mHz}$  with an applied ac potential of  $0.01 \text{ V}$ . The overoxidation process was carried out applying  $0.58 \text{ V}$  at the working electrode for  $60 \text{ min}$ . Therefore, at  $0.3 \text{ V}$  the film is in its oxidized state but there is no electrochemical degradation during the EIS experiment. Before each collection of data, the film was cycled 10 times as described above. We ensured the attainment of a steady electrochemical state in the cell by waiting  $15 \text{ min}$  between the application of the dc potential and recording

the data. Waiting for this time, current passing through the electrochemical cell attains undetectable values. This procedure produces a homogeneous distribution of counterions inside the film. A potentiostatic/galvanostatic Autolab model PGSTAT30 was used for the CV and EIS experiments. The software used to control the whole system and the acquisition and processing of the data were GPES and FRA, for electropolymerization and CV, and for EIS, respectively.

For the EQCM measurements (EG&G PARC, potentiostat 263A, and a Seiko EG&G PARC quartz crystal analyzer QCA 917 model), the same overoxidation process described for EIS was used. A quartz crystal with resonant frequency of 9 MHz was used, and the proportionality factor used for the calculation of the mass from the frequency was 0.858 ng/Hz determined using the method previously described.<sup>20,21</sup> FEG-SEM images were performed with a Zeiss model Supra 35 using polypyrrole electrodes before and after the degradation process.

### 3. RESULTS AND DISCUSSION

Figure 2 shows the CVs obtained for Ppy film during the whole degradation process. We can observe the typical voltammogram pattern which was described in the literature.<sup>22–24</sup> During the scan toward more positive potentials, from  $-0.7$  to  $0.5$  V, polymer oxidation is observed. In the reverse sweep, a reduction peak appears at  $-0.2$  V. As expected, the polymeric film loses its redox capability as the number of voltammetric cycles increases, which is revealed by the decrease in current, attaining an undetectable current after 40 min of electrochemical degradation. As described by Tamm et al.,<sup>25</sup> the differences that appear among the voltammograms could be related to anion mobility changes; i.e., when the ions have high mobility, they are able to leave the polymer during reduction and can be inserted during oxidation. However, as degradation occurs, the authors proposed that the anion mobility inside the polymeric film is damaged. To explain the changes during electrochemical degradation, in this work electrochemical impedance spectroscopy has been applied. Using this technique, we can separate different processes occurring in the sample, such as ionic conductivity in the pore, charge transfer in the polymer/pore solution interface, and electronic conductivity in the polymer chain.

Figure 2b shows the results of the Ppy degradation process followed EIS experiments. As described in the experimental part, all data were collected at  $0.3$  V after a degradation step at  $0.58$  V for different polarization times. At first glance, two important changes are observed in Figure 2b. (i) There is a huge increase in the system resistance, as an increase in the real-part impedance extrapolation of the low-frequency semicircle is observed. Such increase could be related to the polymer, or the polymer/solution interface, or even solution in the pore changes. Therefore, further investigation will be necessary to calculate which one is more probable. (ii) The second important change is a decrease in the low-frequency pseudocapacitance, which could be related to the charge storage in the polymer matrix.<sup>26</sup>

To build a physical description of the electrochemical degradation process, we started the data analysis using a simple double-channel transmission line, which is presented in Figure 3b. In this model, both polymer chains and ion in the pore solution are as described by Ohm's law and the interface among them is a general electrochemical interface with a capacitance and resistance in parallel. As can be observed in Figure 3a, this model cannot correctly describe the data. To improve the model, we

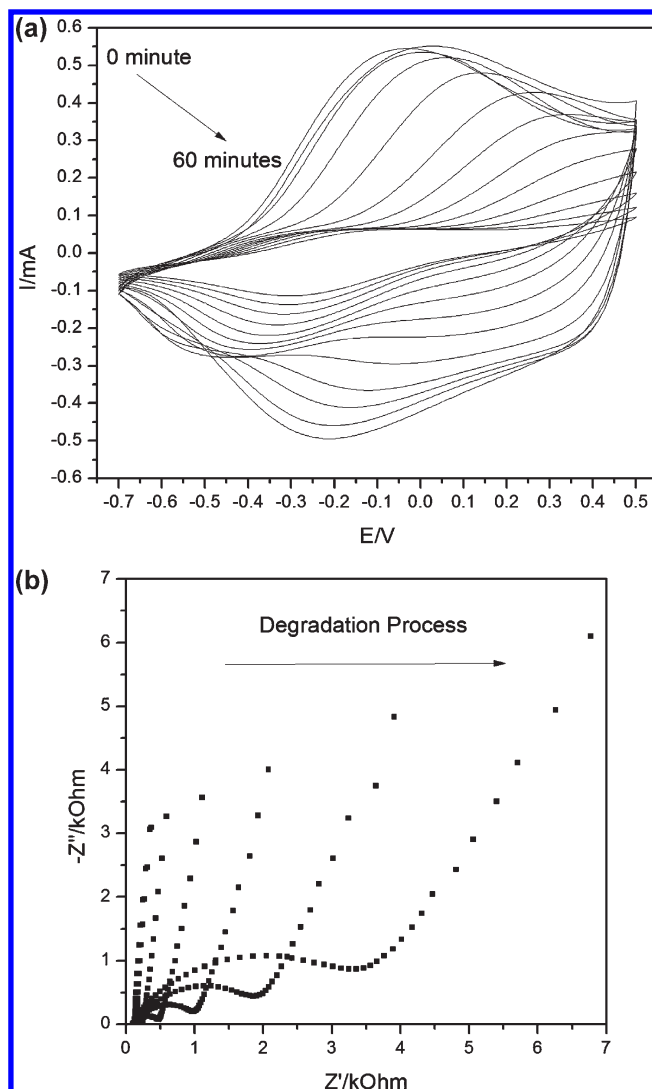


**Figure 2.** (a) Cyclic voltammograms of Ppy film in  $0.1 \text{ mol L}^{-1} \text{ LiClO}_4$  at  $v = 50 \text{ mV s}^{-1}$  after overoxidation at  $0.58 \text{ V}$  for different times in the range from 0 to 60 min. (b) EIS data obtained at  $0.3 \text{ V}$  measured after each voltammogram cycle.

used the approach proposed in the literature stating that ion transport in the pores occurs by diffusion but considering also the existence of trap sites inside them due to their channel width. This kind of diffusion transport has been called anomalous diffusion and has been used to describe the ion transport in different materials.<sup>16,17,27</sup> The model is represented in Figure 3c and the data fitting are also presented in Figure 3a. As can be observed, this model is a better approximation than the first one, yet it cannot completely describe the data. Garcia-Belmonte et al.<sup>26</sup> propose a model in which ion intercalation cannot be associated to a simple charge-transfer resistance. Instead, the authors considered that the ionic charge transfer across the polymer–solution interface could occur far away from an intercalation site in the polymer backbone. Therefore, after an ion crosses the solution–polymer interface, for a period of time there still remains a charge accumulation that could be described by a capacitive process. In other words, an ion could cross the interface anywhere but it needs to reach a stable intercalation site after this step. This model is represented in Figure 3d, and, as can



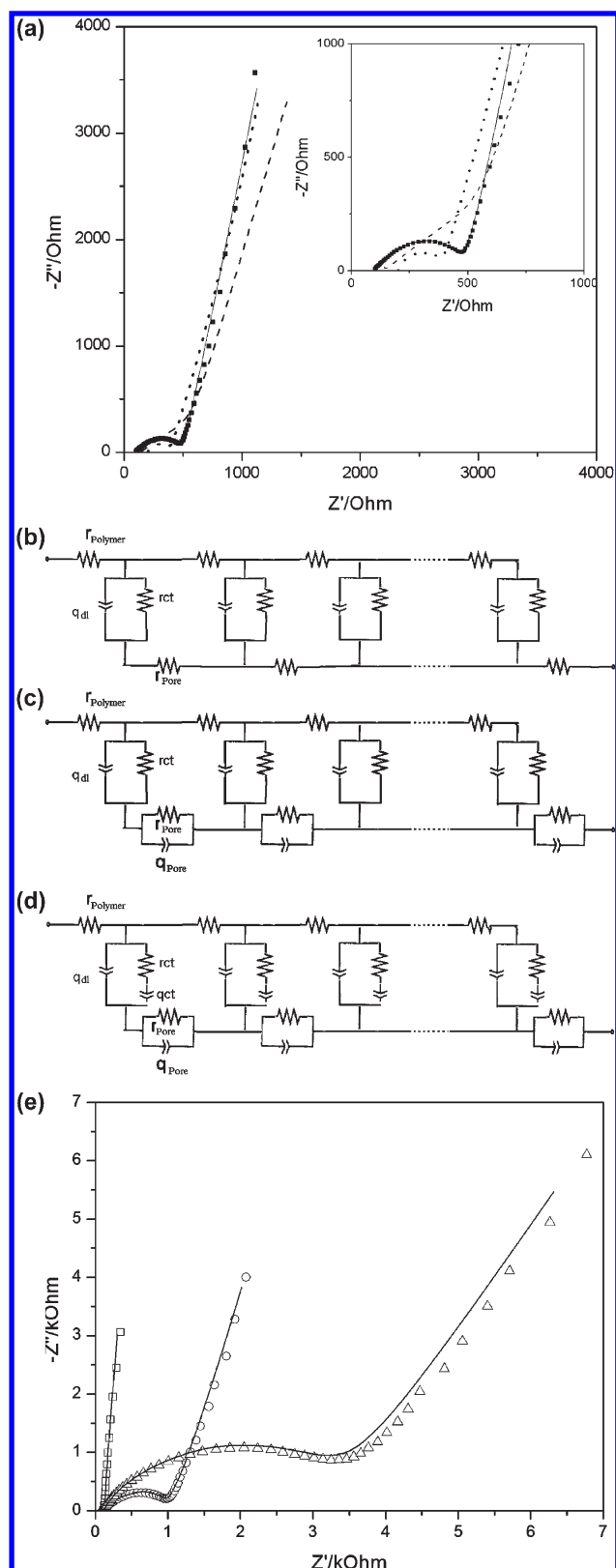


**Figure 3.** (a) Nyquist plot for the polymeric film measured at 0.3 V (■) and fitted results using different transmission line models. Fitting using (---) model (b), (····) model (c), and (—) model d. (e) Nyquist plot for data and fitted results after different overoxidation time at 0.58 V. (□) 0 min, (○) 40 min, and (Δ) 60 min. All measurement were performed in 0.1 mol L<sup>-1</sup> LiClO<sub>4</sub>.

**Table 1.** Parameter Values Obtained from the Degradation Process of the Polypyrrole Electrode Using the Transmission Line Described in Figure 3d

	0 min	10 min	20 min	30 min	40 min	50 min	60 min
$r_{\text{pol}}/\Omega \text{ cm}^{-1}$	16.8	8.05	23.0	18.9	17.5	17.4	24.4
$q_{\text{dl}}/10^{-4} \text{ F s}^{n-1} \text{ cm}^{-1}$	5.40	5.05	1.26	0.83	0.80	0.79	0.41
$n_{\text{dl}}$	0.79	0.77	0.85	0.85	0.97	0.65	0.68
$r_{\text{ct}}/\Omega \text{ cm}$	8.19	26.5	96.5	265	475	1545	2777
$q_{\text{ct}}/10^{-3} \text{ F s}^{n-1} \text{ cm}^{-1}$	4.35	4.31	4.02	3.28	2.59	1.75	1.02
$n_{\text{ct}}$	0.99	0.99	0.94	0.88	0.84	0.78	0.67
$q_{\text{pore}}/10^{-4} \text{ F s}^{n-1} \text{ cm}$	8.20	0.54	2.16	2.29	0.23	0.58	0.12
$n_{\text{pore}}$	0.78	0.65	0.32	0.32	0.41	0.69	0.75
$r_{\text{pore}}/\Omega \text{ cm}^{-1}$	37.5	96.1	220	574	1683	1579	1907

be observed, there is very good adjustment between the experimental and calculated data (Figure 3a).

Comparing Figure 3d with Figure 1,  $\chi_2$  represents the polymer resistance ( $r_{\text{pol}}$ ),  $\chi_1$  is associated with the anomalous ion diffusion in the pores, and the polymer/solution interface  $\zeta$  is represented by a double-layer capacitance ( $q_{\text{dl}}$ ) in parallel with the charge-transfer resistance ( $r_{\text{ct}}$ ), which is in series with the charge-transfer capacitance ( $q_{\text{ct}}$ ), which represents the delay that the anion has to find a stable site to intercalate. Therefore, using the model above, we have obtained excellent fit quality, meaning that the chi-square between data and fit was 0.9999. The model quality was also checked using  $F$  test and it is observed a value greater than  $1 \times 10^5$  for all measurements (see Table 1). It is also presented in Figure 3e, the experimental and fitted data for different degradation treatments 0, 40, and 60 min.

Of course, the good fit adjustment, besides high correlation coefficient and  $F$  values, is not a proof of the model's validity. Besides, it is necessary for the behavior of the calculated parameters to have physical values and convincing changes during the degradation process. Therefore, in the next paragraphs, we discuss the behavior of the calculated parameters. In Figure 4 is shown the variation of the double-layer CPE as the electrochemical degradation process occurs. A strong decrease is observed in their values, which could be explained by a decrease of the exposed surface area between polymer film and solution in the pore. Figure 4b,c supports these conclusions once SEM micrographs before and after the degradation process clearly show a shrink in polymer volume. The macropores observed for the degraded material could be associated with the shrink of the polymer layers.

During the oxidation, positively charged sites are generated in the polymer chain. To compensate the charge, anions must be transferred from the electrolyte in the pores to the polymer across the interface. Therefore, in order to represent these intrinsic, spatially distributed processes, a distributed charge-transfer resistance is necessary, as illustrated here by  $r_{\text{ct}}$ .<sup>28</sup> Figure 5 shows the variation of the charge transfer,  $r_{\text{ct}}$ , and polymer,  $r_{\text{pol}}$ , resistances as the electrochemical degradation occurs.

The huge increase in  $r_{\text{ct}}$  indicates that the process of ion insertion in the polymer matrix has been hindered. As consequence, the loss of reversibility of conducting polymer properties could be related to such a decrease of the intercalation process as proposed by Tamm.<sup>25</sup> Then, as the degraded polymer could no longer intercalate anions, the positive polarons (or bipolarons) are also unstable. Finally, the polymer electrochemical activity decreases as can be observed in Figure 2. An important point

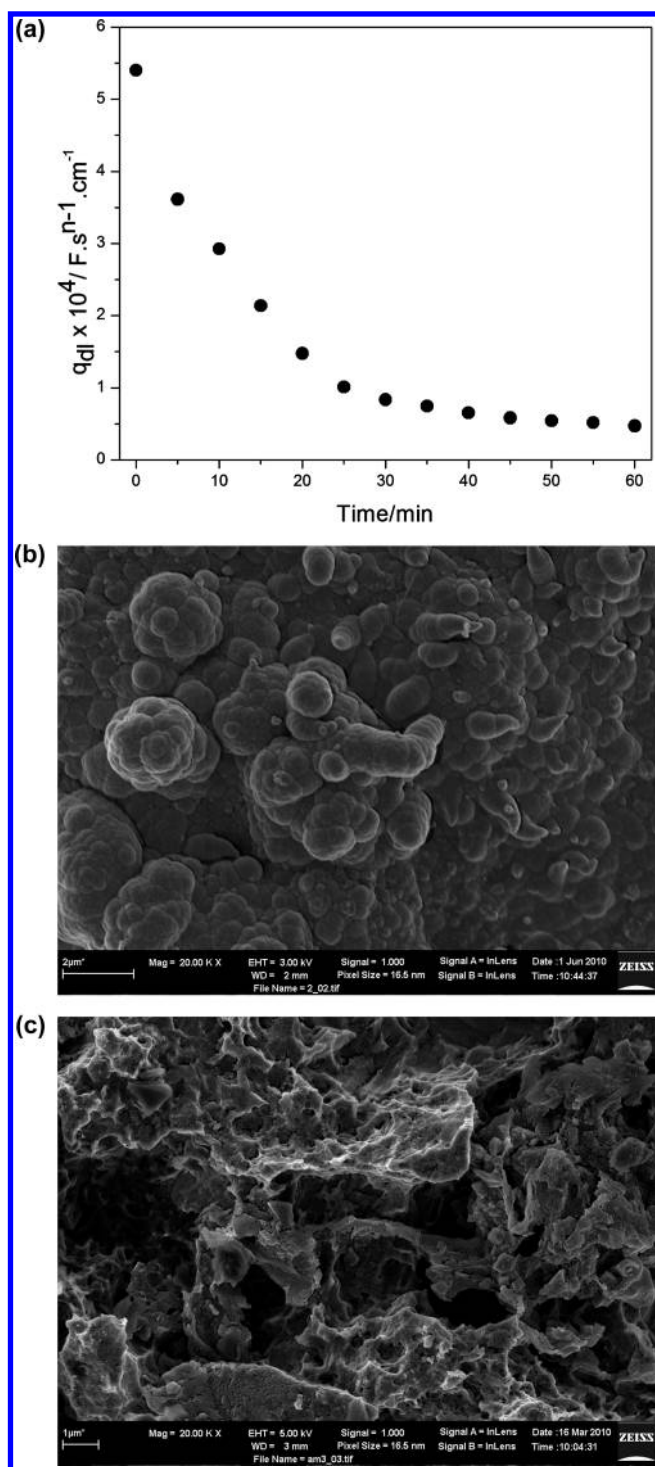


**Figure 4.** (a) Double-layer CPE,  $q_{dl}$ , calculated using model 3d as a function of overoxidation time for polypyrrole in 0.1 mol L<sup>-1</sup> LiClO<sub>4</sub>. SEM images of the polypyrrole electrode after (b) 0 min and (c) 60 min of overoxidation at 0.58 V.

observed in Figure 5 is that the electronic conductivity of the polymer film ( $r_{pol}$ ) does not change as the electrochemical degradation occurs. In this sense, one could propose two different possible degradation mechanisms for a conductive polymer: (i) it arises from electronic conductivity degradation with the bond breaking in the polymer chains and concomitant

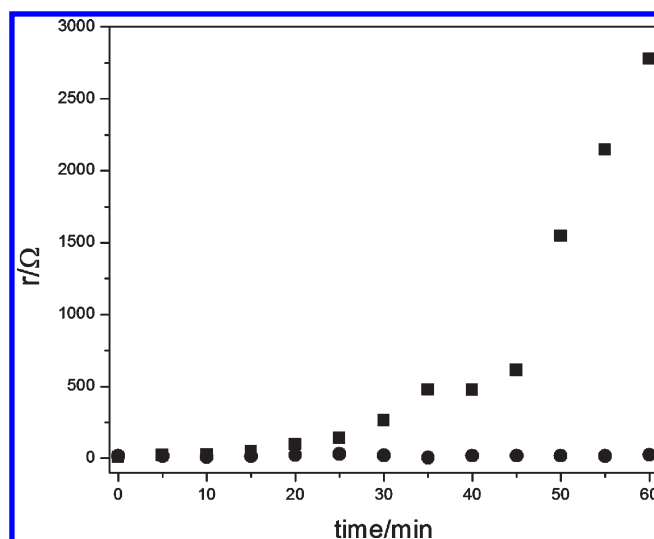


**Figure 5.** Charge-transfer (■) and electric polymer (●) resistances as a function of the degradation process.

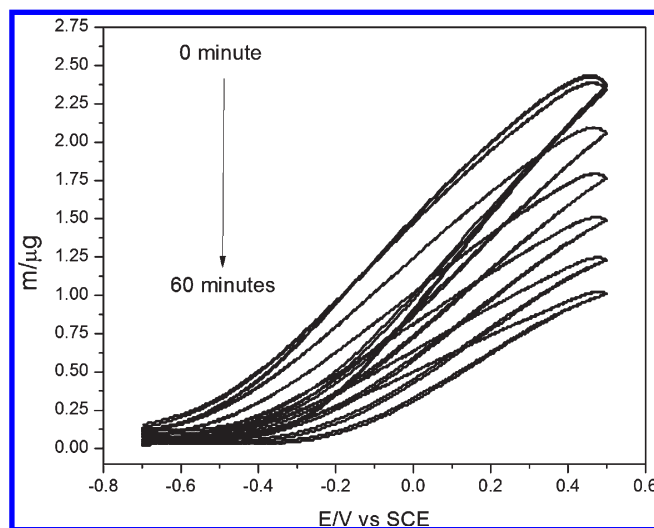


**Figure 6.** EQCM measurements for the polypyrrole film as a function of the degradation process.

generation of soluble species leading to a significant loss of polymer mass and appearance of C–OH and C=O functional groups in the polymer backbone, as well as formation of CO<sub>2</sub> at sufficiently positive potentials;<sup>1</sup> and (ii) a second hypothesis is an electrochemical degradation, as the change in the properties is related to an increase in the energy necessary for ion intercalation as proposed by Palacios.<sup>29</sup> In order to clarify which proposition is most probable, EQCM measurements were performed (Figure 6). These measurements are sensible only to ions intercalation/desintercalation process.

It is observed that, as the degradation process takes place, the mass change of the polymeric film decreases, showing that the loss of electrochemical properties is closely related to ion insertion in the polymer matrix. Therefore, these data corroborate those EIS ones and allow proposing that the electrochemical degradation is probably associated to a decrease in the ion insertion during overoxidation of the polymer.

Otero et al.<sup>30</sup> obtained similar results, where the authors observed degradation in the electroactivity in the polypyrrole film by successive overoxidation treatments by voltammetry and chronoamperometry. The authors found a parallel evolution between the charge needed per cycle to degrade the polymer and the decrease in the diffusion coefficient, suggesting the increasing resistance of the material for ionic interchange during electrochemical processes, in this case, explained by EIS results where a huge increase of the charge-transfer resistance was observed. They also found that a sharp increase in the degradation percentage when the degradation charge per cycle decreases with a growing number of degradation cycles suggested that rigid islands entrapped by cross-linking points might be formed and thereby hinder ionic interchange, which, in this case, is represented by the mass variation loss showed by the EQCM results.

#### 4. CONCLUSIONS

Two different possibilities were considered to explain electrochemical degradation in polypyrrole: electrical degradation and electrochemical degradation. In the former, the main characteristic is the breaking of polymer chains resulting in carbon dioxide formation as well as C–O bonds and cross-linking between neighboring polymer chains and, in the latter, a morphological change in the polymer matrix results in the loss of electrochemical properties of the polymer film. Both degradations result in conductivity loss. Therefore, the electrical degradation could occur in parallel with the electrochemical one, the applied overpotential being the major factor playing the role between them.

In this work, the application of an overpotential in the polymeric film resulted in electrochemical degradation. This was confirmed by EIS, where a transmission line model was applied in order to analyze the results. The main characteristic of a polymeric overoxidation is the damage in the process of ion insertion in the polymer matrix, which results in considerable change in the elements of charge transfer in the polymer/solution interface ( $r_{ct}$  and  $q_{ct}$ ). As the degradation process takes place, the insertion of ions is hindered, and an important change in  $r_{ct}$  is observed. This mechanism is supported by EQCM measurements, which clearly show a decrease in the ion intercalation as the degradation occurs.

#### AUTHOR INFORMATION

##### Corresponding Author

\*E-mail: ernesto@power.ufscar.br.

#### ACKNOWLEDGMENT

The authors acknowledge the assistance of Fundação de Amparo à Pesquisa do Estado de São Paulo (FAPESP), Conselho Nacional de Desenvolvimento Científico e Tecnológico (CNPq), and Coordenação de Aperfeiçoamento Pessoal de Nível Superior (CAPES) in the form of financial support and scholarships.

#### REFERENCES

- (1) Rodríguez, I.; Scharifker, B. R.; Mostany, J. J. *Electroanal. Chem.* **2000**, *491*, 117–125.
- (2) Debiemme-Chouvy, C.; Tran, T. T. M. *Electrochem. Commun.* **2008**, *10*, 947–950.

- (3) Li, Y.; Qian, R. *Electrochim. Acta* **2000**, *45*, 1727–1731.
- (4) Bull, R. A.; Fan, F. F.; Bard, A. J. *J. Electrochem. Soc.* **1982**, *129*, 1009.
- (5) Novak, P.; Vielstich, W. J. *Electrochem. Soc.* **1990**, *137*, 1681.
- (6) Beck, F.; Braun, P.; Oberst, M. *Ber. Bunsenges. Phys. Chem.* **1987**, *91*, 967.
- (7) Schlenoff, J. B.; Xu, H. J. *Electrochem. Soc.* **1992**, *139*, 2397.
- (8) Ge, H.; Qi, G.; Kang, E.; Neoh, K. G. *Polymer* **1994**, *35*, 504.
- (9) Mostany, J.; Scharifker, B. R. *Synth. Met.* **1997**, *87*, 179–185.
- (10) Ramanavicius, A.; Finkelsteinas, A.; Cesiulis, H.; Ramanaviciene, A. *Bioelectrochemistry* **2010**, *79*, 11–16.
- (11) Paasch, A. *Electrochim. Acta* **2002**, *47*, 2049–2053.
- (12) Barcia, O. E.; D'Elia, E.; Frateur, I.; Mattos, O. R.; Pèbère, N.; Tribollet, B. *Electrochim. Acta* **2002**, *47*, 2109–2116.
- (13) De Levie, R. *Adv. Electrochem. Electrochem. Eng.* **1967**, *6*, 329.
- (14) Paasch, G. J. *Electroanal. Chem.* **2007**, *600*, 131–141.
- (15) Shoa, T.; Madden, J. D. W.; Munce, N. R.; Yang, V. *Polym. Int.* **2010**, *59*, 343–351.
- (16) Bisquert, J.; Garcia-Belmonte, G.; Fabregat-Santiago, F.; Compte, A. *Electrochem. Commun.* **1999**, *1*, 429.
- (17) Garcia-Belmonte, G.; Bisquert, J.; Pereira, E. C.; Fabregat-Santiago, F. J. *Electroanal. Chem.* **2001**, *508*, 48–58.
- (18) Warren, M. R.; Madden, J. D. J. *Electroanal. Chem.* **2006**, *590*, 76–81.
- (19) Gabrielli, C.; Perrot, H.; Rubin, A.; Pham, M. C.; Piro, B. *Electrochem. Commun.* **2007**, *9*, 2196–2201.
- (20) Bruckenstein, S.; Swathirajan, S. *Electrochim. Acta* **1985**, *30*, 851.
- (21) Bergamaski, F. O. F.; Santos, M. C.; Nascente, P. A. P.; Bulhões, L. O. S.; Pereira, E. C. J. *Electroanal. Chem.* **2005**, *583*, 162–166.
- (22) Khalkhali, R. A. *Russ. J. Electrochem.* **2005**, *41*, 950–955.
- (23) Tamm, J.; Johanson, U.; Marandi, M.; Tamm, T.; Tamm, L. *Russ. J. Electrochem.* **2004**, *40*, 344–348.
- (24) Varela, H.; Malta, M.; Torresi, R. M. J. *Power Sources* **2001**, *92*, 50–55.
- (25) Tamm, J.; Alumaa, A.; Hallik, A.; Johanson, U.; Tamm, L.; Tamm, T. *Russ. J. Electrochem.* **2002**, *38*, 210–216.
- (26) Garcia-Belmonte, G.; Bisquert, J. *Electrochim. Acta* **2002**, *47*, 4263–4272.
- (27) Garcia-Belmonte, G.; Bisquert, J.; Pereira, E. C.; Fabregat-Santiago, F. *Appl. Phys. Lett.* **2001**, *78*, 1885.
- (28) Rossberg, K.; Paasch, G.; Dunsch, L.; Ludwig, S. J. *Electroanal. Chem.* **1998**, *443*, 49–62.
- (29) López-Palacios, J.; Muños, E.; Heras, M. A.; Colina, A.; Ruiz, V. *Electrochim. Acta* **2006**, *52*, 234–239.
- (30) Otero, T. F.; Márquez, M.; Suárez, I. J. *J. Phys. Chem. B* **2004**, *108*, 15429–15433.